Acta Crystallographica Section F
Structural Biology Communications
ISSN 2053-230X

Purification, crystallization and preliminary crystallographic analysis of Gan1D, a GH1 6-phospho-β-galactosidase from *Geobacillus stearothermophilus* T1

Shifra Lansky,[a] Arie Zehavi,[b] Roie Dann,[a] Hay Dvir,[c] Hassan Belrhali,[d] Yuval Shoham[b]* and Gil Shoham[a]*

[a]Institute of Chemistry and the Laboratory for Structural Chemistry and Biology, The Hebrew University of Jerusalem, Jerusalem 91904, Israel, [b]Department of Biotechnology and Food Engineering, Technion – Israel Institute of Technology, Haifa 32000, Israel, [c]Technion Center for Structural Biology, The Lorry I. Lokey Interdisciplinary Center for Life Science and Engineering, Technion – Israel Institute of Technology, Haifa 32000, Israel, and [d]European Molecular Biology Laboratory, Grenoble Outstation, and Unit for Virus–Host Cell Interactions, European Synchrotron Radiation Facility, Université Grenoble Alpes–EMBL–CNRS, 6 Rue Jules Horowitz, 38042 Grenoble, France

Correspondence e-mail: yshoham@technion.ac.il, gil2@vms.huji.ac.il

Received 3 December 2013
Accepted 28 December 2013

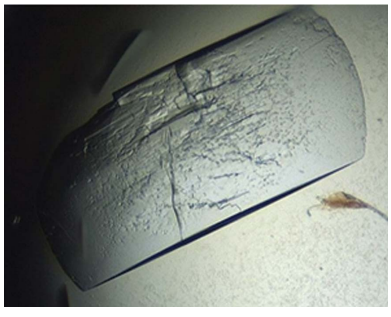

Geobacillus stearothermophilus T1 is a Gram-positive thermophilic soil bacterium that contains an extensive system for the utilization of plant cell-wall polysaccharides, including xylan, arabinan and galactan. The bacterium uses a number of extracellular enzymes that break down the high-molecular-weight polysaccharides into short oligosaccharides, which enter the cell and are further hydrolyzed into sugar monomers by dedicated intracellular glycoside hydrolases. The interest in the biochemical characterization and structural analysis of these proteins originates mainly from the wide range of their potential biotechnological applications. Studying the different hemicellulolytic utilization systems in *G. stearothermophilus* T1, a new galactan-utilization gene cluster was recently identified, which encodes a number of proteins, one of which is a GH1 putative 6-phospho-β-galactosidase (Gan1D). Gan1D has recently been cloned, overexpressed, purified and crystallized as part of its comprehensive structure–function study. The best crystals obtained for this enzyme belonged to the triclinic space group $P1$, with average crystallographic unit-cell parameters of $a = 67.0$, $b = 78.1$, $c = 92.1$ Å, $\alpha = 102.4$, $\beta = 93.5$, $\gamma = 91.7^\circ$. A full diffraction data set to 1.33 Å resolution has been collected for the wild-type enzyme, as measured from flash-cooled crystals at 100 K, using synchrotron radiation. These data are currently being used for the detailed three-dimensional crystal structure analysis of Gan1D.

1. Introduction

6-Phospho-β-galactosidases (EC 3.2.1.85) are enzymes that hydrolyze the β-glycosidic bond between a terminal nonreducing galactose-6-phosphate and other organic molecules. These enzymes are usually associated with the phosphotransferase system (PTS transport system), an alternative intake system involved in the transport and phosphorylation of numerous monosaccharides, disaccharides, amino sugars, polyols and a series of other sugar derivatives. These unique PTS transport systems, also referred to as phosphoenolpyruvate–carbohydrate phosphotransferase systems (PEP-PTS), are only found in bacteria (Postma *et al.*, 1993; Robillard & Broos, 1999; Deutscher *et al.*, 2006). According to the CAZy database, all of the 6-phospho-β-galactosidases reported to date belong to family 1 of the glycoside hydrolases (GH1; Henrissat & Davies, 1997) and seem to act *via* a retaining mechanism. Based on sequence analysis, 6-phospho-β-galactosidases are identified to be involved in lactose utilization in *Staphylococcus aureus*, *Lactococcus lactis*, *Lactobacillus casei* and *Streptococcus mutans* (de Vos & Gasson, 1989; Breidt & Stewart, 1987; Porter & Chassy, 1988; Honeyman & Curtiss, 1993). In these bacteria, lactose is transported into the cell and phosphorylated *via* a phosphotransferase system and further hydrolyzed inside the cell by a 6-phospho-β-galactosidase, resulting in glucose and galactose 6-phosphate (Breidt *et al.*, 1987; de Vos *et al.*, 1990; Alpert & Chassy, 1990; Rosey & Stewart, 1992). Only a small number of these enzymes have been biochemically characterized, most of them in lactic bacteria such as *Lactococcus lactis*, *Lactobacillus gasseri* and *Streptococcus lactis* (McKay *et al.*, 1970; Suzuki *et al.*, 1996*a*,*b*; Honda *et al.*, 2012). Of these enzymes, only the 6-phospho-β-galactosidase from *L. lactis* has been subjected to full crystallographic analysis (Wiesmann *et al.*, 1995, 1997).

Geobacillus stearothermophilus is a thermophilic, Gram-positive, soil bacterium which possesses an extensive system for the utilization of plant cell-wall polysaccharides, including xylan, arabinan and galactan (Shulami *et al.*, 1999, 2011; Tabachnikov & Shoham, 2013). The bacterium secretes a small number of extracellular enzymes that cleave high-molecular-weight polysaccharides into shorter decorated oligosaccharides. The resulting oligosaccharides are transported into the cell *via* specialized ABC transporters (Rees *et al.*, 2009) and are further hydrolyzed into sugar monomers by a battery of specific intracellular glycoside hydrolases. The most studied and the best characterized of these complex utilization systems is that of xylan, where the bacterium secretes an extracellular xylanase (Gat *et al.*, 1994; Teplitsky *et al.*, 1997, 2004; Bar *et al.*, 2004) that partially degrades xylan to short decorated xylooligosaccharides, which are then transported into the cell *via* dedicated ABC transporters (Shulami *et al.*, 2007). Inside the cell, the decorated xylooligosaccharides are hydrolyzed by several side-chain-cleaving enzymes, including arabinofuranosidases (Shallom, Belakhov, Solomon, Gilead-Gropper *et al.*, 2002; Shallom, Belakhov, Solomon, Shoham *et al.*, 2002; Hövel *et al.*, 2003), an α-glucuronidase (Teplitsky *et al.*, 1999; Golan *et al.*, 2004; Zaide *et al.*, 2001; Shallom *et al.*, 2004), acetylesterases (Alalouf *et al.*, 2011; Lansky, Alalouf *et al.*, 2013; Lansky *et al.*, 2014) and finally by an intracellular xylanase (Teplitsky *et al.*, 2000; Solomon *et al.*, 2007) and several xylosidases (Bravman *et al.*, 2003; Shallom *et al.*, 2005; Brüx *et al.*, 2006; Ben-David *et al.*, 2007).

In the framework of a wider study of the hemicellulolytic utilization systems in *G. stearothermophilus* T1, we have characterized a galactan-utilization gene cluster in this bacterium (Tabachnikov & Shoham, 2013). This 9.4 kb cluster includes several transcriptional units, which encode, among other proteins, an extracellular galactanase (Gan53A), an intracellular galactosidase (Gan42B) (Solomon *et al.*, 2013) and a specific ABC sugar transporter (GanEFG) (Tabachnikov & Shoham, 2013). It is therefore suggested that Gan53A cleaves the high-molecular-weight polymer galactan outside of the cell into galactooligosaccharides; these oligosaccharides are then transported *via* the ABC sugar transport system into the cell, where they are further hydrolyzed to galactose by Gan42B. In addition to this system, we recently identified another 12.5 kb gene cluster that, based on real-time RT-PCR analysis, is induced by galactan and galactose, suggesting that this cluster is also involved in the utilization of galactan (unpublished results). The newly discovered cluster includes five transcriptional units, which encode a putative GH1 6-phospho-β-galactosidase (Gan1D), a transcriptional regulator (GanR2), a GH4 6-phospho-β-glucosidase (Gan4C), a three-component regulatory system (GanPST) and another dedicated ABC sugar transport system (GanE2F2G2). Relatively little is known about these five protein components, except that the ABC transporter seems to recognize galactose and that the sugar-binding lipoprotein of the three-component regulatory system, GanP, has been shown to bind both galactose and glucose (unpublished results).

The current study is part of a larger project geared to characterize in detail the proteins involved in this new transport system, both alone and as an integrated cellular system. In the present report, we describe the purification, crystallization and preliminary crystallographic characterization of one of these proteins, Gan1D, as the first step toward its three-dimensional structural determination and the corresponding structure–function analysis. As a key player in the biochemical hydrolysis of polymeric β-1,4-galactosaccharides into galactose monomers, Gan1D and related enzymes play an important part of the hemicellulolytic utilization system of many microorganisms which use plant biomass for growth. The interest in the biochemical characterization and structural analysis of these enzymes stems therefore not only from basic scientific interest, but also from their numerous potential biotechnological applications.

2. Experimental

2.1. Cloning, expression and purification of Gan1D

The *gan1D* gene was amplified *via* PCR fused to a six-His-tag extrapeptide at its N-terminus and was cloned into pET-9d (Novagen, Madison, Wisconsin, USA). The gene was amplified from chromosomal DNA of *G. stearothermophilus* T1 using PCR, based on the genomic sequence (GenBank accession No. KF840174, base pairs 236–1672). The PCR primers were Gan1D N-ter, 5′-TATAG**TCATG**-**A**TACATCACCACCACCACCATGAGCATCGTCATCTTAAAC-3′, which included a His_6 tag and a *Bsp*HI restriction site (TCATGA), and Gan1D C-ter, 5′-TATAC**GGATCC**CTACAGCTCGGCACCGT TC-3′, which included a *Bam*HI restriction site (GGATCC). The PCR product was digested with the appropriate restriction enzymes and cloned into pET-9d vector linearized with *Nco*I and *Bam*HI to give pET-9d-*gan1D*. Expression of *gan1D* was carried out by growing *Escherichia coli* BL21 (λDE3) cells (Stratagene, La Jolla, California, USA) harbouring pET-9d-*gan1D* in 2 l shake flasks containing 0.5 l Terrific broth medium supplemented with 25 µg ml^{-1} kanamycin, which were shaken at 230 rev min^{-1} at 310 K. Following overnight growth (final $OD_{600\ nm}$ of about 13), cells from 1 l culture were harvested, resuspended in 40 ml buffer (20 m*M* imidazole, 20 m*M* phosphate buffer, 500 m*M* NaCl pH 7.0), disrupted by two passages through an Avestin Emulsiflex C3 Homogenizer (Avestin) and centrifuged (14 000 rev min^{-1} for 30 min) to obtain soluble extract. The His-tagged fused protein was isolated using a 5 ml HisTrap column (GE Healthcare Life Sciences) mounted on an ÄKTA Avant-25 chromatography system (GE Healthcare Life Sciences) according to the manufacturer's instructions. The final protein sample was more than 95% pure, based on SDS–PAGE, with a total yield of approximately 50 mg per litre of overnight culture. Gel-permeation chromatography on a Superose 12 column (GE Healthcare Life Sciences) indicated that the native protein has a molecular weight of about 110 kDa.

2.2. Biochemical experiments

The activity of Gan1D towards various substrates has been qualitatively determined in a number of preliminary experiments using a continuous colorimetric assay. The reactions were performed at 313 K in 100 mm citric acid–Na_2HPO_4 buffer pH 7.6, 0.5 *M* NaCl, 1 mg ml^{-1} BSA and 10 µg ml^{-1} Gan1D. Substrate concentrations were in the range 0–35 m*M*. The reactions were initialized by adding 50 µl of appropriately diluted (within the range 0.1–10 K_m) pre-warmed substrate to 150 µl pre-warmed enzyme solution in a 96-well plate. The absorbance at 405 nm was measured at 30 s intervals for 20 min using a Synergy HT Multi-Mode Microplate Reader (Bio-Tek Instruments, Winooski, Vermont, USA).

2.3. Crystallization experiments

Crystallization experiments were set up immediately after the last purification step of the recombinant wild-type Gan1D protein. The purified protein was concentrated to approximately 4 mg ml^{-1} using Centricon centrifugal concentrators (Millipore, Massachusetts, USA) and this protein solution was used for the crystallization experiments. All initial crystallization experiments were performed by the hanging-drop vapour-diffusion method, using an extensive series of different factorial screens (Jancarik & Kim, 1991). In general, these

initial conditions were based on commercially available sets of 'ready-to-use' screening solutions. Once positive results had been obtained (*i.e.* crystals or microcrystals), further refinement experiments of these crystallization conditions were performed with specially prepared solutions, optimizing parameters such as pH, ionic strength, protein concentration, temperature, precipitating additives, protein drop volume and drop-to-reservoir ratio (Almog *et al.*, 1993, 1994; Teplitsky *et al.*, 1997, 1999, 2000; Bar *et al.*, 2004; Lansky, Alalouf *et al.*, 2013; Lansky, Salama *et al.*, 2013; Solomon *et al.*, 2013).

The final Gan1D protein crystallization drops were prepared by mixing the concentrated protein solution (2.0–3.0 µl, ∼4 mg ml^{-1}) with an equal amount of each of the specific screen solutions to give a final drop volume of 4.0–6.0 µl. Each of these protein drops was suspended over 0.5–1.0 ml reservoir solution in 4 × 6 VDX crystallization plates (Hampton Research, California, USA) for a period of about 1–8 d at a constant temperature of 293 K. One of these initial screening experiments resulted in reasonable crystals (in terms of size and shape) and fine refinement of this condition resulted in two different crystal forms. As explained below, although the two crystal forms showed reasonable X-ray diffraction properties, only one of them was found to be suitable for further crystallographic analysis at high resolution.

Most of the X-ray diffraction data measurements were performed at the European Synchrotron Research Facility (ESRF), Grenoble, France. Processing, reduction, indexing, integration and scaling of the synchrotron diffraction data were conducted using the *HKL*-2000 program package (Otwinowski & Minor, 1997). Some of the crystals were further analyzed at the Technion Center for Structural Biology (TCSB), Technion, Haifa, Israel, using our in-house X-ray source (see below). Processing, reduction, indexing, integration and scaling of the TCSB diffraction data were conducted using the programs *iMosflm* (Battye *et al.*, 2011) and *SCALA* (Evans, 2006).

3. Results and discussion

3.1. Preliminary characterization of Gan1D

The *gan1D* gene is part of a 12.5 kb cluster that is upregulated when *G. stearothermophilus* T1 grows on galactose as the sole carbon source. The gene encodes a 478-amino-acid protein with a calculated molecular mass of 55 204 Da. Based on *BLAST* analysis, Gan1D shows more than 35% sequence homology to a number of GH1 6-phospho-β-galactosidases, including those from *L. lactis* (37% sequence identity), *S. aureus* (38%), *S. mutans* (37%) and *L. casei* (36%), and the GH1 6-phospho-β-glucosidases from *Lactobacillus plantarum* (39% sequence identity) and *S. mutans* (37%) (de Vos & Gasson, 1989; Breidt & Stewart, 1987; Porter & Chassy, 1988; Honeyman & Curtiss, 1993; Michalska *et al.*, 2013). The 6-phospho-β-galactosidases and 6-phospho-β-glucosidases show relatively high sequence similarity to each other. However, using the reported crystal structures of the GH1 6-phospho-β-galactosidase from *L. lactis* and the GH1 6-phospho-β-glucosidases from *L. plantarum* and

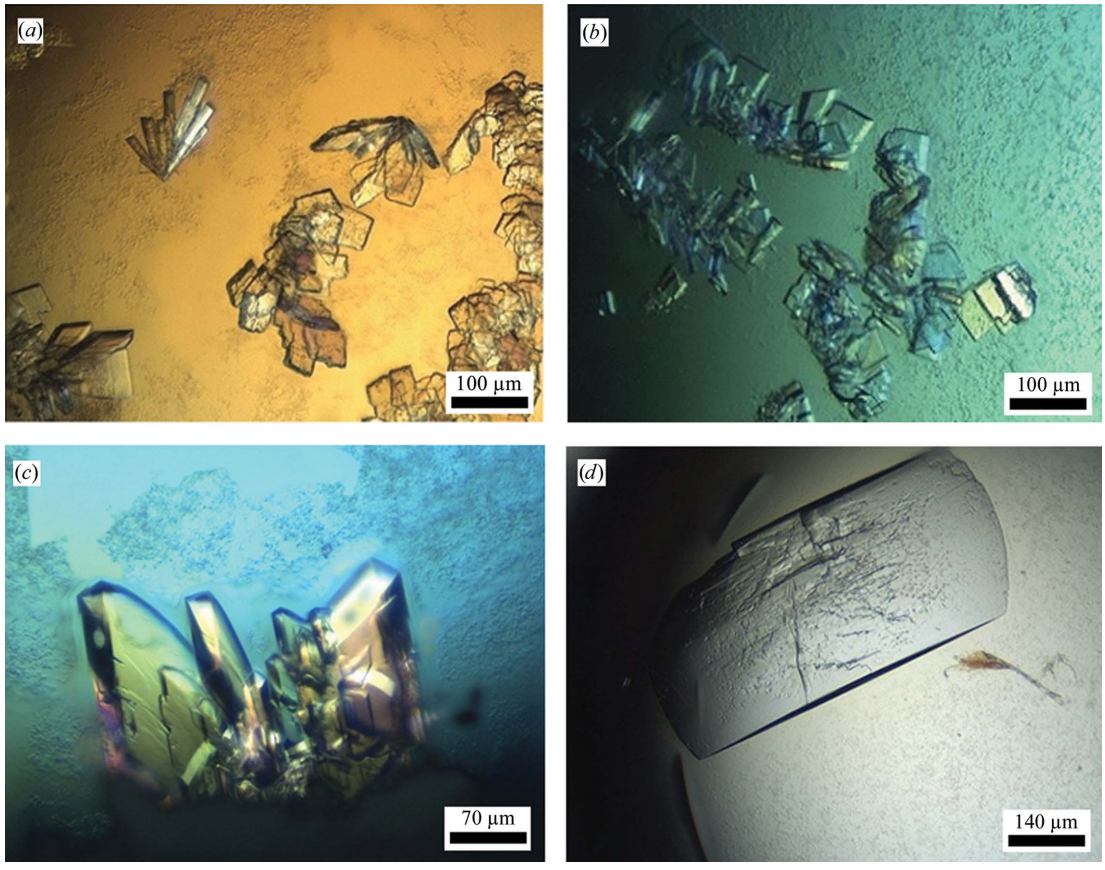

Figure 1
Crystals of the two habits obtained for Gan1D. (*a*–*c*) Typical crystals of the EFP habit. It is noted that crystals of the EFP habit vary in shape between elongated rectangular bars (*a*, top left), almost perfect square boxes (*b*, top centre), flat rectangular plates (*a*, right; *b*, bottom) and various polyhedral prisms (*a*, *b*, *c*). They also vary in size from typically around 0.05 × 0.05 × 0.01 mm (*a*, *b*) to sometimes as large as 0.12 × 0.07 × 0.03 mm (*c*). Larger crystals of the type presented in (*c*) were used for the measurement of the full diffraction data set described here at 1.33 Å resolution (Fig. 2). (*d*) A typical crystal of the RP habit, with dimensions of around 0.7 × 0.4 × 0.05 mm.

S. mutans, it should be possible, in principle, to predict the preferred activity of GH1 enzymes of this type based only on their three-dimensional structure (Wiesmann *et al.*, 1997; Michalska *et al.*, 2013). In the 6-phospho-β-galactosidase from *L. lactis* the key residue Trp429 is localized in the phosphate-binding pocket, at a hydrogen-bonding distance from the axial position of the O4 hydroxyl group of a bound galactose (Wiesmann *et al.*, 1997). In the 6-phospho-β-glucosidases this Trp residue is replaced by an Ala (Ala431 in *L. plantarum*), which clashes with the axial O4 hydroxyl group of galactose 6-phosphate but not with the equatorial O4 hydroxyl group of glucose 6-phosphate (Michalska *et al.*, 2013). Since Gan1D contains the Trp433 residue in this position (based on sequence alignment), it is suggested that the enzyme is likely to be a 6-phospho-β-galactosidase.

The *gan1D* gene was readily overexpressed in the *E. coli* pET system, and gel-permeation chromatography of the purified protein suggested that the native protein is a dimer in solution, with a molecular mass of about 110 kDa per dimer. As noted above, relatively little is presently known about Gan1D and its catalytic properties. In a series of preliminary experiments, however, Gan1D exhibited residual activity towards 4-nitrophenyl β-D-galactopyranoside and 2-nitrophenyl β-D-glucopyranoside, and significantly higher activity towards 4-nitrophenyl β-D-glucose 6-phosphate and 4-nitrophenyl β-D-galactose 6-phosphate. These experiments support our initial assignment of Gan1D as a 6-phospho-β-galactosidase, which was based only on its sequence homology and its observed genetic regulation.

3.2. Crystal forms of wild-type Gan1D

The preliminary screening experiments were based on several commercial screens, including Crystal Screen and Crystal Screen 2 (Hampton Research, California, USA), and Wizard Classic Screens 1–4 (Emerald BioSystems, Bainbridge Island, Washington, USA). As noted above, those initial crystallization screens indicated only one condition that produced useful crystals. This was solution No. 39 of the Wizard Classic 4 Screen, consisting of 20%(*w*/*v*) polyethylene glycol 8000 (PEG 8K), 3%(*v*/*v*) (±)-2-methyl-2,4-pentanediol (MPD), 0.1 *M* imidazole buffer pH 6.5. This initial condition was further refined, resulting in two slightly different crystallization conditions that differed from each other only by the total content of the PEG component and the exact concentration of the protein. In condition 1, the initial protein concentration was around 3.9–4.3 mg ml^{-1} and the reservoir solution (and half of the protein crystallization drop) consisted of 16–18%(*w*/*v*) PEG 8K, 3%(*v*/*v*) MPD, 0.1 *M* imidazole buffer pH 6.48. In condition 2, the initial protein concentration was around 4.3–4.5 mg ml^{-1} and the reservoir solution contained the same general components but with 19–22% rather than 16–18% PEG 8K. Surprisingly, this relatively small difference in the PEG component led to two different crystal forms. The crystals obtained from condition 1 usually appeared as small elongated flat prisms (EFP habit), varying in the shape of the flat face from elongated triangles to elongated rectangles (Figs. 1*a*, 1*b* and 1*c*). The typical dimensions of the EFP crystals were in the range 0.05–0.12 × 0.02–0.07 mm for the flat face, with a thickness of around 0.01–0.03 mm (Figs. 1*a* and 1*b*). These crystals appeared usually in clusters of three to eight crystals, all originating from a common crystallization core. In some of the drops it was possible to isolate single, nonclustered crystals of this form, some of which were used for the detailed crystallographic characterization and data collection described below. The crystals obtained from condition 2 usually appeared as larger rectangular plates (RP habit), with typical dimensions in the range 0.4–0.7 × 0.2–0.4 × 0.01–0.05 mm (Fig. 1*d*). Although larger in overall size, the RP crystals usually appeared in multiple layers (Fig. 1*d*), making it difficult to isolate a suitable single monolayered crystal for crystallographic analysis.

Table 1
Representative parameters for the crystallographic data of Gan1D.

Values in parentheses are for the outer resolution shell.

Protein crystal	Gan1D (EFP habit)	Gan1D (RP habit)
X-ray system	ESRF BM14	Technion TCSB
Wavelength (Å)	0.979	1.54
Space group	*P*1	*C*2
Resolution range (Å)	40.0–1.33 (1.35–1.33)	40.0–1.92 (2.03–1.92)
Unit-cell parameters		
a (Å)	67.0	108.0
b (Å)	78.1	68.9
c (Å)	92.1	152.9
α (°)	102.4	90
β (°)	93.5	100.7
γ (°)	91.7	90
No. of reflections		
Total	2986976	264862
Unique	429175	86922
Multiplicity	3.9 (3.8)	3.2 (3.1)
$\langle I\rangle/\langle\sigma(I)\rangle$	11.9 (2.4)	6.0 (2.3)
Mosaicity (°)	0.32	0.69
Completeness (%)	95.5 (92.3)	99.7 (98.5)
$R_{\rm merge}$† (%)	5.5 (59.6)	10.4 (32.3)

† $R_{\rm merge} = \sum_{hkl}\sum_i |I_i(hkl) - \langle I(hkl)\rangle|/\sum_{hkl}\sum_i I_i(hkl)$, where $I_i(hkl)$ is the intensity of observation i of reflection hkl.

3.3. Crystallographic characterization of the RP crystal habit

The X-ray diffraction pattern of the RP crystals indicated that they belong to a *C*-centred monoclinic crystal system (space group *C*2), with average unit-cell parameters of a = 108.0, b = 68.9, c = 152.9 Å, β = 100.7°. Using a synchrotron setup (ESRF beamline BM14) the best crystals of this form displayed detectable X-ray diffraction to a resolution limit of around 1.8 Å, but with smeared spots and relatively large overall mosaicity values. In comparison (at the time), the EFP crystals proved to be more suitable for crystallographic structural analysis (see below), as based on the reproducibility of the crystallization experiments, handling and cooling of the resulting crystals and the quality of the diffraction pattern obtained. At this point, it was therefore decided to continue further crystallographic studies (at the ESRF) mainly with this type of crystals, as further described in §§3.4 and 3.5.

At a later point (after the full characterization of the EFP crystals), we decided to further characterize the RP crystals for use as potential 'back-up' crystals for future enzyme–substrate structural studies, if needed. These crystallographic analyses were performed at the TCSB, using an FR-X rotating-anode (Rigaku, Japan) X-ray source (λ = 1.54 Å) coupled to an R-AXIS HTC (Rigaku, Japan) detector and an Oxford Cryosystem crystal-cooling system (100 K). Several crystals of this form (from different crystallization batches) have been examined, some of which proved to be quite reasonable for crystallographic analysis. One such RP Gan1D crystal (Fig. 1*d*) was used for a full X-ray diffraction data measurement to 1.92 Å resolution. This oscillation data set included 555 frames, measured with a $\Delta\varphi$ of 0.3°, 2 min exposure time per frame and a crystal-to-detector distance of 140 mm. The raw diffraction images were processed with *iMosflm* (Battye *et al.*, 2011) and scaled with *SCALA* (Evans, 2006). A total of 264 862 reflections were measured in the 40.00–1.92 Å resolution range and resulted in 86 922 independent reflections, with 99.7% overall completeness to 1.92 Å resolution and 98.5% completeness for the highest resolution shell (2.03–1.92 Å). The overall diffraction

multiplicity of the processed data set was 3.2, the overall mosaicity was 0.69°, the mean $I/\sigma(I)$ was 6.0 and the final $R_{\rm merge}$ for the whole data was 10.4%. These parameters indicate that the data collected from the RP crystal represent a reasonable diffraction data set that could potentially be used as a basis for crystal structure analysis (Table 1). These parameters confirm, however, that the EFP crystals are preferable over the RP crystals for high-resolution structural studies of the Gan1D protein, as demonstrated in detail below.

3.4. Crystallographic characterization of the EFP crystal habit

After refinement of the initial conditions, it was determined that the best conditions for obtaining EFP Gan1D crystals are those of the general hanging-drop procedure described above using a protein concentration of 4.3 µg µl^{-1} and a reservoir solution consisting of 17%(*w*/*v*) PEG 8K, 3% MPD, 0.1 *M* imidazole buffer pH 6.48. In these conditions, a larger portion of the resulting crystals appeared as single crystals or as small clusters of relatively thick crystals (Fig. 1*c*) that were rather easy to break into single crystals.

Several such EFP Gan1D crystals were used for a detailed crystallographic characterization and measurement of X-ray diffraction data under cryogenic conditions. These experiments were performed using X-ray synchrotron radiation (λ = 0.979 Å) and a CCD area detector (MAR 225, MAR Research, USA) on the BM14 beamline of the ESRF. The crystal-cooling procedure used for these experiments included a short soak of the selected crystal (for about 20–60 s) in a cryoprotecting solution consisting of 30%(*w*/*v*) PEG 4K, 14%(*w*/*v*) PEG 8K, 3%(*v*/*v*) MPD, 0.1 *M* imidazole buffer pH 6.48. Each of these pre-soaked crystals was then submitted to a flash-cooling procedure by immediate immersion in liquid nitrogen followed by quick transfer into the centre of a cold nitrogen-gas stream (100 K; Oxford Cryosystem), which flowed around the crystal throughout the X-ray data collection.

The observed diffraction pattern of some of these crystals exceeded the 1.4 Å resolution limit and indicated that the crystals belonged to the triclinic crystal system (space group *P*1), with average crystallographic unit-cell parameters of a = 67.0, b = 78.1, c = 92.1 Å, α = 102.4, β = 93.5, γ = 91.7°. Different crystals of this crystallization batch gave similar unit-cell parameters, with an overall deviation from these average values of less than 0.2%.

3.5. X-ray diffraction data for Gan1D

One such Gan1D crystal was used for a full X-ray diffraction data measurement to 1.33 Å resolution (Fig. 2). This oscillation data set included 360 frames, measured with a $\Delta\varphi$ of 1°, 5 s exposure and a crystal-to-detector distance of 114.3 mm on the BM14 beamline at the ESRF, as described above (λ = 0.979 Å, 100 K). The raw CCD diffraction images were processed with the *HKL*-2000 software package (Otwinowski & Minor, 1997). A total of 2 986 976 accepted reflections [$F > 0\sigma(F)$] were measured in the 40.00–1.33 Å resolution range and resulted in 429 175 independent reflections with 95.5% overall completeness to 1.33 Å resolution and 92.3% completeness for the highest resolution shell (1.35–1.33 Å). The overall diffraction multiplicity of the processed data set was 3.9, the overall mosaicity value was 0.32°, the average $I/\sigma(I)$ was 11.9 and the final $R_{\rm merge}$ for the whole data set was 5.5% (59.6% for the highest resolution shell). These parameters confirm that the data collected represent an almost complete diffraction data set of relatively high quality (Table 1).

A rough calculation of the specific ratio of volume/protein ($V_{\rm M}$) was performed in order to estimate the number of protein monomers per crystallographic asymmetric unit. The volume of the Gan1D crystallographic unit cell, as determined from the mean value of the unit-cell parameters at 100 K, is 4.83 × 10^5 Å^3. Assuming that the $V_{\rm M}$ and the overall water content values here are within the normal range observed for soluble proteins (Matthews, 1968; Kantardjieff & Rupp, 2003), there should be either three or four molecules of Gan1D monomers (478 amino-acid residues, molecular mass 55 204 Da per monomer) in the crystallographic asymmetric unit. With three molecules in the *P*1 asymmetric unit (and the unit cell), the calculated

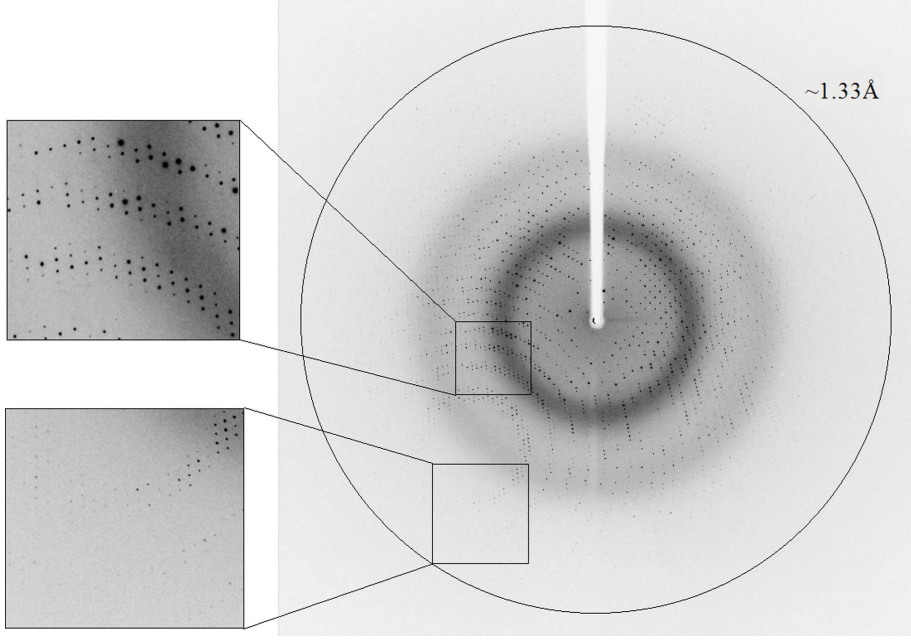

Figure 2
X-ray diffraction pattern of the Gan1D crystals (EFP habit), obtained using a synchrotron source (BM14, ESRF). The outer circle corresponds to a 1.33 Å resolution limit. The insets represent magnified views of the sections indicated by the corresponding squares (top, medium resolution; bottom, high resolution).

V_M is 2.92 Å^3 Da^{-1} and the corresponding solvent content in the crystals is 57.9%. With four molecules in the asymmetric unit, the calculated V_M is 2.19 Å^3 Da^{-1} and the corresponding solvent content in the crystals is 43.8%. Both of these two possibilities seem to be reasonable considering their calculated V_M values and water content. However, according to the gel-filtration results, Gan1D appears to be a dimer in solution (see above), making the second possibility the more likely solution, featuring two homodimers of Gan1D in the *P*1 unit cell. The presence of two protein dimers per unit cell was also supported by self-rotation calculations.

This full 1.33 Å resolution data set should now be used for the detailed three-dimensional structural analysis of Gan1D. A search in the Protein Data Bank (PDB) indicated two relevant three-dimensional protein structures that share more than 40% sequence identity with Gan1D. One of these proteins is a β-glucosidase from *Streptomyces* sp. (PDB entry 1gnx, 1.68 Å resolution, 42% sequence identity; A. Guasch, M. Vallmitjana, R. Perez, E. Querol, J. A. Perez-Pons & M. Coll, unpublished work). The second protein is a β-glucosidase from *Bacillus circulans* sp. *alkalophilus* (PDB entry 1qox, 2.7 Å resolution, 41% sequence identity; Hakulinen *et al.*, 2000). Also relevant is the structure of the 6-phospho-β-galactosidase from *L. lactis*, for which a full crystallographic analysis has been performed at 2.3 Å resolution (PDB entries 1pbg and 4pbg; 37% sequence identity; Wiesmann *et al.*, 1995, 1997). These three structures could be used now as suitable reference models for molecular-replacement calculations, which are expected to solve the phase problem and provide good starting models for the full structural analysis of the Gan1D protein. Such analyses are currently in progress in our laboratory.

This work was supported by the Israel Science Foundation Grants 500/10 and 152/11, the I-CORE Program of the Planning and Budgeting Committee, the Ministry of Environmental Protection and the Grand Technion Energy Program (GTEP), and comprises part of The Leona M. and Harry B. Helmsley Charitable Trust reports on Alternative Energy series of the Technion, Israel Institute of Technology and the Weizmann Institute of Science. YS acknowledges the core services and support from the Lorry I. Lokey Center for Life Sciences and Engineering and the Russell Berrie Nanotechnology Institute, Technion. We thank the staff at the European Synchrotron Research Facility (ESRF beamline BM14) for their helpful support in the X-ray synchrotron data measurement and analysis. The synchrotron experiments at the ESRF were also supported by the ESRF internal funding program. HD thanks the European Union's Seventh Framework Programme (FP7/2007-2013) under grant agreement No. 330879-MC-CHOLESTRUCTURE for financial support. YS holds the Erwin and Rosl Pollak Chair in Biotechnology at the Technion.

References

Alalouf, O., Balazs, Y., Volkinshtein, M., Grimpel, Y., Shoham, G. & Shoham, Y. (2011). *J. Biol. Chem.* **286**, 41993–42001.

Almog, O., Greenblatt, H. M., Spungin, A., Ben-Meir, D., Blumberg, S. & Shoham, G. (1993). *J. Mol. Biol.* **230**, 342–344.

Almog, O., Klein, D., Braun, S. & Shoham, G. (1994). *J. Mol. Biol.* **235**, 760–762.

Alpert, C. A. & Chassy, B. M. (1990). *J. Biol. Chem.* **265**, 22561–22568.

Bar, M., Golan, G., Nechama, M., Zolotnitsky, G., Shoham, Y. & Shoham, G. (2004). *Acta Cryst.* D**60**, 545–549.

Battye, T. G. G., Kontogiannis, L., Johnson, O., Powell, H. R. & Leslie, A. G. W. (2011). *Acta Cryst.* D**67**, 271–281.

Ben-David, A., Bravman, T., Balazs, Y. S., Czjzek, M., Schomburg, D., Shoham, G. & Shoham, Y. (2007). *Chembiochem*, **8**, 2145–2151.

Bravman, T., Zolotnitsky, G., Belakhov, V., Shoham, G., Henrissat, B., Baasov, T. & Shoham, Y. (2003). *Biochemistry*, **42**, 10528–10536.

Breidt, F. Jr, Hengstenberg, W., Finkeldei, U. & Stewart, G. C. (1987). *J. Biol. Chem.* **262**, 16444–16449.

Breidt, F. Jr & Stewart, G. C. (1987). *Appl. Environ. Microbiol.* **53**, 969–973.

Brüx, C., Ben-David, A., Shallom-Shezifi, D., Leon, M., Niefind, K., Shoham, G., Shoham, Y. & Schomburg, D. (2006). *J. Mol. Biol.* **359**, 97–109.

Deutscher, J., Francke, C. & Postma, P. W. (2006). *Microbiol. Mol. Biol. Rev.* **70**, 939–1031.

Evans, P. (2006). *Acta Cryst.* D**62**, 72–82.

Gat, O., Lapidot, A., Alchanati, I., Regueros, C. & Shoham, Y. (1994). *Appl. Environ. Microbiol.* **60**, 1889–1896.

Golan, G., Shallom, D., Teplitsky, A., Zaide, G., Shulami, S., Baasov, T., Stojanoff, V., Thompson, A., Shoham, Y. & Shoham, G. (2004). *J. Biol. Chem.* **279**, 3014–3024.

Hakulinen, N., Paavilainen, S., Korpela, T. & Rouvinen, J. (2000). *J. Struct. Biol.* **129**, 69–79.

Henrissat, B. & Davies, G. (1997). *Curr. Opin. Struct. Biol.* **7**, 637–644.

Honda, H., Nagaoka, S., Kawai, Y., Kemperman, R., Kok, J., Yamazaki, Y., Tateno, Y., Kitazawa, H. & Saito, T. (2012). *J. Gen. Appl. Microbiol.* **58**, 11–17.

Honeyman, A. L. & Curtiss, R. III (1993). *J. Gen. Microbiol.* **139**, 2685–2694.

Hövel, K., Shallom, D., Niefind, K., Baasov, T., Shoham, G., Shoham, Y. & Schomburg, D. (2003). *Acta Cryst.* D**59**, 913–915.

Jancarik, J. & Kim, S.-H. (1991). *J. Appl. Cryst.* **24**, 409–411.

Kantardjieff, K. A. & Rupp, B. (2003). *Protein Sci.* **12**, 1865–1871.

Lansky, S., Alalouf, O., Solomon, V., Alhassid, A., Govada, L., Chayan, N. E., Belrhali, H., Shoham, Y. & Shoham, G. (2013). *Acta Cryst.* F**69**, 430–434.

Lansky, S., Alalouf, O., Solomon, V., Alhassid, A., Govada, L., Chayen, N. E., Belrhali, H., Shoham, Y. & Shoham, G. (2014). *Acta Cryst.* D**70**, doi:.10.1107/S139900471302840X.

Lansky, S., Salama, R., Solomon, V. H., Belrhali, H., Shoham, Y. & Shoham, G. (2013). *Acta Cryst.* F**69**, 695–699.

Matthews, B. W. (1968). *J. Mol. Biol.* **33**, 491–497.

McKay, L., Miller, A. III, Sandine, W. E. & Elliker, P. R. (1970). *J. Bacteriol.* **102**, 804–809.

Michalska, K., Tan, K., Li, H., Hatzos-Skintges, C., Bearden, J., Babnigg, G. & Joachimiak, A. (2013). *Acta Cryst.* D**69**, 451–463.

Otwinowski, Z. & Minor, W. (1997). *Methods Enzymol.* **276**, 307–326.

Porter, E. V. & Chassy, B. M. (1988). *Gene*, **62**, 263–276.

Postma, P. W., Lengeler, J. W. & Jacobson, G. R. (1993). *Microbiol. Rev.* **57**, 543–594.

Rees, D. C., Johnson, E. & Lewinson, O. (2009). *Nature Rev. Mol. Cell Biol.* **10**, 218–227.

Robillard, G. T. & Broos, J. (1999). *Biochim. Biophys. Acta*, **1422**, 73–104.

Rosey, E. L. & Stewart, G. C. (1992). *J. Bacteriol.* **174**, 6159–6170.

Shallom, D., Belakhov, V., Solomon, D., Gilead-Gropper, S., Baasov, T., Shoham, G. & Shoham, Y. (2002). *FEBS Lett.* **514**, 163–167.

Shallom, D., Belakhov, V., Solomon, D., Shoham, G., Baasov, T. & Shoham, Y. (2002). *J. Biol. Chem.* **277**, 43667–43673.

Shallom, D., Golan, G., Shoham, G. & Shoham, Y. (2004). *J. Bacteriol.* **186**, 6928–6937.

Shallom, D., Leon, M., Bravman, T., Ben-David, A., Zaide, G., Belakhov, V., Shoham, G., Schomburg, D., Baasov, T. & Shoham, Y. (2005). *Biochemistry*, **44**, 387–397.

Shulami, S., Gat, O., Sonenshein, A. L. & Shoham, Y. (1999). *J. Bacteriol.* **181**, 3695–3704.

Shulami, S., Raz-Pasteur, A., Tabachnikov, O., Gilead-Gropper, S., Shner, I. & Shoham, Y. (2011). *J. Bacteriol.* **193**, 2838–2850.

Shulami, S., Zaide, G., Zolotnitsky, G., Langut, Y., Feld, G., Sonenshein, A. L. & Shoham, Y. (2007). *Appl. Environ. Microbiol.* **73**, 874–884.

Solomon, H. V., Tabachnikov, O., Feinberg, H., Govada, L., Chayen, N. E., Shoham, Y. & Shoham, G. (2013). *Acta Cryst.* F**69**, 1114–1119.

Solomon, V., Teplitsky, A., Shulami, S., Zolotnitsky, G., Shoham, Y. & Shoham, G. (2007). *Acta Cryst.* D**63**, 845–859.

Suzuki, M., Saito, T. & Itoh, T. (1996*a*). *Biosci. Biotechnol. Biochem.* **60**, 139–141.

Suzuki, M., Saito, T. & Itoh, T. (1996*b*). *Biosci. Biotechnol. Biochem.* **60**, 708–710.

Tabachnikov, O. & Shoham, Y. (2013). *FEBS J.* **280**, 950–964.

Teplitsky, A., Feinberg, H., Gilboa, R., Lapidot, A., Mechaly, A., Stojanoff, V., Capel, M., Shoham, Y. & Shoham, G. (1997). *Acta Cryst.* D**53**, 608–611.

Teplitsky, A., Mechaly, A., Stojanoff, V., Sainz, G., Golan, G., Feinberg, H., Gilboa, R., Reiland, V., Zolotnitsky, G., Shallom, D., Thompson, A., Shoham, Y. & Shoham, G. (2004). *Acta Cryst.* D**60**, 836–848.

Teplitsky, A., Shulami, S., Moryles, S., Shoham, Y. & Shoham, G. (2000). *Acta Cryst.* D**56**, 181–184.
Teplitsky, A., Shulami, S., Moryles, S., Zaide, G., Shoham, Y. & Shoham, G. (1999). *Acta Cryst.* D**55**, 869–872.
Vos, W. M. de, Boerrigter, I., van Rooyen, R. J., Reiche, B. & Hengstenberg, W. (1990). *J. Biol. Chem.* **265**, 22554–22560.
Vos, W. M. de & Gasson, M. J. (1989). *J. Gen. Microbiol.* **135**, 1833–1846.
Wiesmann, C., Beste, G., Hengstenberg, W. & Schulz, G. E. (1995). *Structure*, **3**, 961–968.
Wiesmann, C., Hengstenberg, W. & Schulz, G. E. (1997). *J. Mol. Biol.* **269**, 851–860.
Zaide, G., Shallom, D., Shulami, S., Zolotnitsky, G., Golan, G., Baasov, T., Shoham, G. & Shoham, Y. (2001). *Eur. J. Biochem.* **268**, 3006–3016.